

# Molecular Imaging of Angiogenesis in Cardiac Regeneration

Ljubica Mandić<sup>1</sup> · Denise Traxler<sup>1</sup> · Alfred Gugerell<sup>1</sup> · Katrin Zlabinger<sup>1</sup> ·  
Dominika Lukovic<sup>1</sup> · Noemi Pavo<sup>1</sup> · Georg Goliasch<sup>1</sup> · Andreas Spannauer<sup>1</sup> ·  
Johannes Winkler<sup>1</sup> · Mariann Gyöngyösi<sup>1</sup>

Published online: 10 September 2016

© The Author(s) 2016. This article is published with open access at Springerlink.com

## Abstract

**Purpose of Review** Myocardial infarction (MI) leading to heart failure displays an important cause of death worldwide. Adequate restoration of blood flow to prevent this transition is a crucial factor to improve long-term morbidity and mortality. Novel regenerative therapies have been thoroughly investigated within the past decades.

**Recent Findings** Increased angiogenesis in infarcted myocardium has shown beneficial effects on the prognosis of MI; therefore, the proangiogenic capacity of currently tested treatments is of specific interest. Molecular imaging to visualize formation of new blood vessels in vivo displays a promising option to monitor proangiogenic effects of regenerative substances.

**Summary** Based on encouraging results in preclinical models, molecular angiogenesis imaging has recently been applied in a small set of patients. This article reviews recent literature on noninvasive in vivo molecular imaging of angiogenesis after MI as an integral part of cardiac regeneration.

**Keywords** Angiogenesis · Myocardial regeneration · Molecular imaging · Integrins · Radiotracers · Myocardial infarction

## Introduction

Heart failure following myocardial infarction (MI) still displays a major cause of death and disability worldwide [1].

Even though a wide range of therapeutic options to prevent or delay transition to chronic heart failure (CHF) after MI are available, its treatment is still unsatisfactory, as CHF is generally not reversible and treatment needs to be continued indefinitely [2]. Angiogenesis, the formation of new blood vessels, is a part of the natural healing process after MI to restore blood flow and discard cellular debris [3]. The extent of angiogenesis is associated with postinfarct remodeling and has implications on prognosis in MI patients [4]. Although a variety of approaches to stimulate myocardial angiogenesis after MI have been explored, including gene therapy as well as the delivery of angiogenic factors and stem cells, results have been controversial and were partly disappointing [5–7]. In many cases, stimulation of angiogenesis was not shown convincingly and only moderate clinical improvement was demonstrated. To reliably assess the therapeutic potential of proangiogenic therapies and monitor myocardial angiogenesis for enabling better preclinical and clinical drug development, noninvasive methods such as molecular imaging are warranted. Molecular imaging of newly built microvessels is a promising strategy which allows direct visualization of vessel formation instead of indirect measurements of efficacy. Thus, it is an important modality for improving risk stratification and for facilitating the development of novel therapeutic interventions in MI patients.

## Angiogenesis

Angiogenesis represents the growth of new capillaries from preexisting vessels [8]. It is a complex process involving numerous growth factors and signal cascades [9]. Although vessels are generally quiescent in adults, endothelial cells (ECs) lining the vessel walls retain their ability to respond to angiogenic signals [8]. Proangiogenic signals such as VEGF, ANG-2, FGFs, or chemokines released by hypoxic, inflammatory, or tumor cells activate ECs, and they become motile and invasive

---

This article is part of the Topical Collection on *Molecular Imaging*

✉ Mariann Gyöngyösi  
mariann.gyongyosi@meduniwien.ac.at

<sup>1</sup> Department of Cardiology, Medical University of Vienna, Waehringer Guertel 18-20, 1090 Vienna, Austria

[10]. Before ECs can sprout into surrounding tissue, degradation of basement membrane by matrix metalloproteases and detachment of mural cells is necessary in order to loosen activated ECs [8]. VEGF induces increased permeability of the EC layer, and extravasated plasma proteins serve as a provisional extracellular matrix (ECM) scaffold. Migration of ECs into this scaffold is mediated by integrins. To allow blood flow, those newly built vessels need to be connected with other vessels to build branches and become mature and stable. ECs regain their quiescent state and protease inhibitors cease basement membrane degradation [10].

Insufficient vessel maintenance can lead to MI [10]. Intact and functional blood vessels are essential for regeneration of ischemic tissues to enable immune surveillance, supply of oxygen and nutrients to and discarding of waste from the cells of the healing wound [10, 11]. Insufficiently healed MI results in an expanded infarction area and dilation of the heart by left ventricular (LV) remodeling, both resulting in heart failure [12]. However, in some patients, recovery of blood flow after MI is not possible. In those patients, restoration of tissue reperfusion depends on myocardial angiogenesis [1]. Within the first hours after MI, proangiogenic factors are released to compensate ischemia with induced angiogenesis [11]. Restoration of the blood flow in the infarct border zone is essential to alleviate infarct expansion and heart failure [1, 13]. Moreover, the extent of angiogenesis has positive effects on postinfarct remodeling and the prognosis of MI patients [4]. Hence, stimulation of myocardial angiogenesis as a therapeutic option through administering growth factors, stem or progenitor cells, and pharmacological molecules has been thoroughly studied [14]. Due to the increasing amount of research on myocardial angiogenesis as a treatment option, molecular imaging of newly built vessels has a significant potential impact on predicting outcome of MI patients and guiding novel therapies.

### Molecular Imaging Tools

Molecular imaging describes *in vivo* targeted, noninvasive visualization and quantification of various molecular pathways without interfering with them [15–18]. Throughout the past decades, there has been significant advances in molecular imaging techniques used for diagnostic, prognostic, as well as therapeutic purposes [18]. In the field of cardiology, molecular imaging by magnetic resonance imaging (MRI), ultrasound, bioluminescence imaging, positron emission tomography (PET), and SPECT has shown improvements of LV function, myocardial perfusion, viability, scar tissue, inflammatory cells, and indirect signs of angiogenesis, and some of these images are able to directly detect angiogenesis [15].

### Nuclear Imaging

PET imaging is a tomographic technique that detects the decay of positron emitters (radiotracers), which can be attached to small molecules for molecular recognition [17, 19]. It is well validated to have superior sensitivity, relatively high resolution, and tissue penetration [1920•]. Various metabolic and pathophysiological biomarkers have been investigated as targets for PET imaging. The nonspecific metabolic tracer  $^{18}\text{F}$  (in form of 18-fluorodeoxyglucose),  $^{18}\text{F}$ -FDG, is the most frequently employed PET tracer [21, 22]. Many studies are directed toward incorporation of radiotracers with short half-lives, such as fluorine-18 ( $^{18}\text{F}$ ), which successfully leads to reduced patient exposure of ionizing radiation [23]. Rather low spatial resolution is the main limiting characteristic of this imaging technique [21].

SPECT imaging is well established and offers several advantages over PET. Camera equipment is less expensive and more widely available as compared to PET systems [23]. SPECT imaging performance is based on using single photon emitting radioisotopes, which are easier accessible for the investigation of a wider range of biological processes [15, 24]. Technetium-99m ( $^{99\text{m}}\text{Tc}$ ) and indium-111 ( $^{111}\text{In}$ ) are frequently used radioactive probes [19]. These radiotracers emit gamma rays with different energies, thus introducing the possibility of simultaneous evaluation of dual or multiple radiotracers. Advantages of SPECT are high sensitivity and tissue penetration depth. However, SPECT imaging does not ensure high-resolution anatomical information of cellular location. Another disadvantage is the inability to track radioisotopes over weeks as the signal rapidly declines [19].

### MRI

In contrast to PET and SPECT, MRI offers better spatial resolution, excellent soft tissue contrast and enables concomitant angiography or perfusion acquisition [21]. However, it has a lower sensitivity for detection of molecular contrast agents and application is limited in patients with devices, e.g., cardiac pacemakers or cardioverter defibrillators, and metal implants [15, 25]. Paramagnetic contrast agents (e.g., gadolinium) targeting integrin  $\alpha_v\beta_3$  via antibodies or peptidomimetics as well as gadolinium-based lipid nanoparticles, have been previously used to study tumor angiogenesis [26–28]. A further advance in MR angiogenesis imaging are ultra-small superparamagnetic particles of iron oxide (USPIO) [29]. However, USPIOs have a long blood half-life and show nonspecific extravasation [30]. Microparticles of iron oxide (MPIO) have a higher particle size, and thus a shorter half-life, offering a better contrast to noise ratio [31]. Safety concerns of superparamagnetic iron oxide particles exist [32].

## Ultrasound Molecular Imaging

Cardiac ultrasound is a widely used technique that has several advantages over the previously described imaging modalities, e.g., lack of ionizing radiation, routine accessibility, and superior spatial resolution compared to SPECT and PET [33]. Hitherto tissue perfusion assessed by ultrasound has been used as an endpoint reflecting angiogenesis; however, an increase in perfusion does not necessarily reflect angiogenic activity [34]. For more detailed imaging, targeted microbubbles can be used as contrast agents in a technique known as contrast-enhanced ultrasound (CEU) [33]. Microbubbles that target integrins or VEGFRs reflect angiogenesis in a more direct manner than perfusion imaging [34, 35].

## Bioluminescence Imaging

Bioluminescence imaging (BLI) represents an indirect cell labeling method particularly used in small animal models [36]. It is greatly valued for its high sensitivity, ease of use, and low cost of instrumentation, but BLI has low spatial resolution and restricted penetration depth, and quantification accuracy is very poor [37, 38]. Most frequently used reporter genes are firefly luciferase (Luc) and herpes simplex virus thymidine kinase (HSV-tk), used for tracking cells with angiogenic capacity [39].

## Multimodal Imaging

Advances in molecular imaging, along with identifying drawbacks, have led to the development of multimodal (hybrid) imaging systems such as PET/MR, SPECT/computed tomography (CT), and PET/CT [18]. Hybrid molecular imaging is the focus of many preclinical and clinical studies as it enables simultaneous collection of anatomical and functional information [40, 41].

The addition of CT to SPECT has permitted attenuation correction and better evaluation of SPECT myocardial perfusion [42]. SPECT/CT has proven to be relevant in the characterization of coronary artery calcium, which is a useful method to predict cardiovascular events rate [43, 44]. Even though SPECT/CT has been widely used in cardiology and information gained with this modality are highly valued, exposure of patients to radiation is a major concern [45] and reduction of radiation is the main goal of present studies in nuclear cardiology [46].

PET/CT is a hybrid technology that combines functional molecular imaging modalities with precise anatomical information [47]. This hybrid modality is successful in overcoming low spatial resolution. Many studies indicate that it results in better identification of diseases, and guide management and treatment of patients with stable and unstable coronary artery disease compared to PET imaging alone [48].

## Molecular Imaging of Myocardial Angiogenesis

Within the past decade, direct noninvasive evaluation of angiogenesis by molecular imaging has been investigated extensively. With the rapid development of antiangiogenic therapies (e.g., in cancer research) and particularly imaging techniques, tumor angiogenesis has been the focus of attention lately [49]. Although interest has recently increasingly been directed on molecular imaging of myocardial angiogenesis after MI (e.g., to monitor effects of regenerative therapies), it is still rather in its fledgling stage. Table 1 provides a summary of novel studies on molecular imaging of angiogenesis.

Angiogenesis as a multistep process, orchestrated by a wide range of growth factors, growth factor receptors, cell types, adhesion molecules, integrins, and signaling pathways, all of which offer a multitude of imaging targets. In general, three ways to image myocardial angiogenesis exist: (1) non-EC targets, (2) EC targets, and (3) extracellular matrix proteins and matrix proteases [58]. In particular, integrin  $\alpha_v\beta_3$  has emerged as an interesting target.

## Integrins

Integrins are structurally and functionally diverse families of cell adhesion molecules, which regulate cell-cell and cell-ECM interactions and in addition mediate signals for cell growth, proliferation, migration, or apoptosis [59]. They connect the ECM with the cytoskeleton (i.e., the microfilaments) inside the cell and transmit signals of the surrounding into the cell by mediating the downstream consequences of cell adhesion. Therefore, integrins play an important role in cell signaling and can have a relation to cell growth, cell division, cell survival, differentiation, and apoptosis [60]. Several members of the integrin family are overexpressed on ECs under hypoxia [61]. The two main integrins  $\alpha_v\beta_3$  and  $\alpha_5\beta_1$  facilitate several mechanisms during angiogenesis in tissue ischemia. In particular, they mediate adhesion to ECM and other cells to initiate building of new capillaries by allowing ECs to bind to provisional ECM scaffold proteins. Furthermore, they mediate interaction of ECs and vascular smooth muscle cells, stimulate vessel growth, and promote vessel maturation [10, 61]. ECM proteins such as fibronectin interact with integrins via the Arg-Gly-Asp (RGD) sequence motif [61]. Multivalent binding is mediated through extracellular integrin clusters, and thus, dimeric and multimeric RGD sequences with improved binding affinity have been developed and are frequently used for integrin imaging.

## Integrin $\alpha_v\beta_3$

Integrin  $\alpha_v\beta_3$ -mediated imaging is currently the most frequently applied method to visualize angiogenesis in vivo. Its expression is low in normal tissue, but it becomes highly

**Table 1** A summary of novel studies in molecular imaging of angiogenesis

	Radiotracer	Modality	Target	Therapy	Species	Disease
Myocardial						
Preclinical	$^{68}\text{Ga}$ -NODAGA-RGD	PET	$\alpha_v\beta_3$ integrin	None	Rat	MI
	$^{68}\text{Ga}$ -TRAP(RGD) <sub>3</sub>					
	$^{18}\text{F}$ -galacto-RGD [50]					
	$^{68}\text{Ga}$ -NOTA-RGD peptidomimetic [51]	PET	$\alpha_v\beta_3$ integrin	None	Rat	MI
	$^{18}\text{F}$ -Alfatide II [20•]	PET	$\alpha_v\beta_3$ integrin	VEGF, BMSC	Rat	MI
	$^{68}\text{Ga}$ -RGD [52•]	PET	$\alpha_v\beta_3$ integrin	Dissociated HUVECs/cbMSCs or 3D HUVEC/cbMSC aggregates	Rat	MI
	$^{111}\text{In}$ -DTPA-cNGR [53]	SPECT	CD13	None	Mouse	MI
	$^{64}\text{Cu}$ -NOTA-TRC105 [54]	PET	CD105	None	Rat	MI
	[ $^{11}\text{C}$ ]ATV-1[9]	PET	VEGFR-2, Tie-2, PDGF $\alpha$	None	Rat	MI
Clinical	$^{68}\text{Ga}$ -PRGD2 [55••]	PET	$\alpha_v\beta_3$ integrin	None	Human	MI
Hind limb						
Preclinical	$\alpha_v$ targeted microbubbles [34]	Ultrasound	$\alpha_v$ integrins	HIF-1 $\alpha$ mutants	Mouse	Ischemic hind limb
Tumor						
	c(RGDyK)-MPIO [56•]	MRI	$\alpha_v\beta_3$ integrin	None	Mouse	Melanoma, colon carcinoma
	$^{68}\text{Ga}$ -aquibepirin [57••]	PET	$\alpha_5\beta_1$ integrin	None	Mouse	melanoma

expressed in activated ECs during angiogenesis in the infarcted myocardium [61, 62]. However, studies in  $\alpha_v$ - and  $\beta_3$ -deficient mice suggest that both integrins are not essentially required for angiogenesis and their absence can be compensated by upregulation of VEGFR-2 expression [63–65]. Additionally, integrin  $\alpha_v\beta_3$  does not seem to be restricted to ECs but is also expressed on macrophages so that results in angiogenesis imaging targeting integrin  $\alpha_v\beta_3$  need to be treated with caution [66].

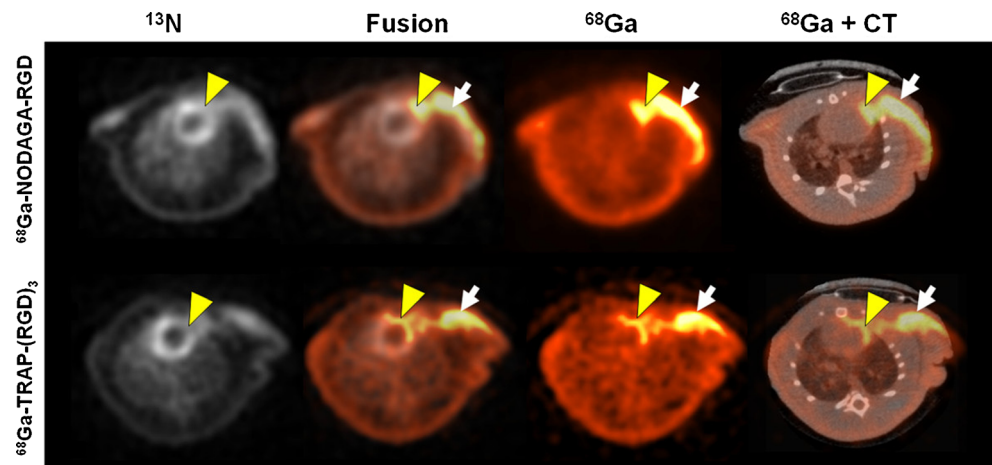
For integrin  $\alpha_v\beta_3$  molecular imaging, cyclic RGD dimers with polyethylene glycol spacers radiolabeled with  $^{18}\text{F}$  [67, 68],  $^{68}\text{Ga}$  [69, 70],  $^{64}\text{Cu}$  [71],  $^{76}\text{Br}$  [72], and  $^{89}\text{Zr}$  [73] for PET imaging and  $^{99\text{m}}\text{Tc}$  [74, 75] and  $^{111}\text{In}$  [76] for SPECT imaging were used in several disease entities. Within the past years, the use of these and other tracer probes that had been investigated predominantly in tumor angiogenesis has been translated to angiogenesis imaging after MI for evaluating proangiogenic effects of regenerative therapies. In a previous study,  $^{18}\text{F}$ -galacto-RGD injected in a rat MI model predicted improved healing [77]. The usage of this tracer, however, might be limited as the production of  $^{18}\text{F}$ -galacto-RGD is complex and time-consuming.  $^{68}\text{Ga}$  tracers, on the other hand, are easy to handle and fast in production.  $^{68}\text{Ga}$ -NODAGA-RGD and  $^{68}\text{Ga}$ -TRAP-(RGD)<sub>3</sub> have been previously tested for angiogenesis imaging in tumor models [78, 79]. Both  $^{68}\text{Ga}$ -RGD tracers were compared to  $^{18}\text{F}$ -galacto-RGD in postinfarct

myocardial angiogenesis, and uptake was similar in all three groups (Fig. 1), indicating that  $^{68}\text{Ga}$ -RGD tracers may represent a more easily clinically translatable alternative [50]. Another  $^{68}\text{Ga}$ -labeled tracer, a  $^{68}\text{Ga}$ -NOTA-RGD peptidomimetic, was used for angiogenesis imaging in a rat MI model.  $^{68}\text{Ga}$ -NOTA-RGD uptake was increased in regions of reduced myocardial perfusion and correlated with immunohistochemical staining of CD31 and  $\beta_3$  integrin (Fig. 2) [51].

Lately,  $^{18}\text{F}$ -Alfatide II ( $^{18}\text{F}$ -AIF-NOTA-PRGD2) has been developed as a new promising PET tracer. Taking advantage of the preformation of an aluminum-fluoride complex with consequent attachment of the RGD peptide, time for preparation was significantly reduced and HPLC purification was avoided, while receiving radiochemical purity of over 97 % [80]. The  $^{18}\text{F}$ -Alfatide II tracer was used to characterize angiogenesis in a rat MI model after treatment with vascular endothelial growth factor (VEGF) gene and/or bone marrow mesenchymal stem cells (BMSCs). In this study,  $^{18}\text{F}$ -Alfatide II provided a strong contrast between infarcted and noninfarcted myocardium and uptake was significantly higher in rats treated with VEGF and BMSCs (Fig. 3). Increased uptake of  $^{18}\text{F}$ -Alfatide II correlated with the area of  $^{99\text{m}}\text{Tc}$ -MIBI uptake defect [20•].

In another study in a rat MI model, the angiogenic potential of 3D HUVEC/cbMSC aggregates was assessed by  $^{68}\text{Ga}$ -

**Fig. 1** In vivo PET/CT images of rat MI. Representative transaxial sections show hypoperfused myocardium area ( $^{13}\text{N}$ ) and corresponding RGD uptake ( $^{68}\text{Ga}$ , % ID/g). The focal uptake is seen in infarct (yellow arrowheads) and the operation scar (white arrows), as verified by CT scan (reprinted from [50] under the terms of the Creative Commons Attribution License 2.0)



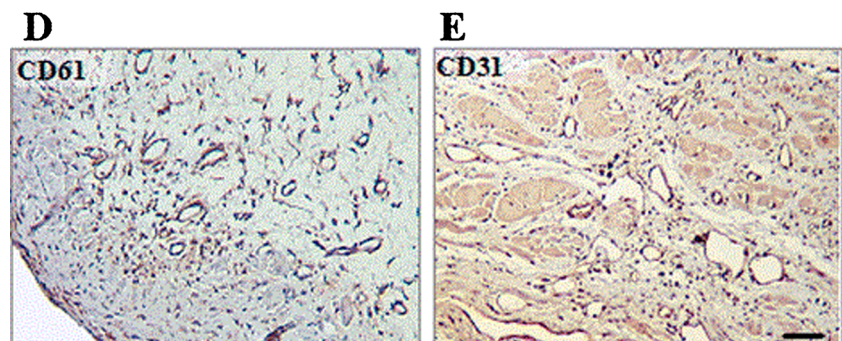
RGD. Injection of 3D HUVEC/cbMSC aggregates resulted in locally increased  $^{68}\text{Ga}$ -RGD uptake suggesting increased angiogenesis and reduction in defect size [52•]. Using SPECT tracers, an increased uptake of  $^{99\text{m}}\text{Tc}$ -labeled RGD peptides ( $^{99\text{m}}\text{Tc}$ -RAFT-RGD and  $^{99\text{m}}\text{Tc}$ -NC100692), similar to data of respective  $^{18}\text{F}$ -PET tracers, was found in infarcted myocardium tissue and the border zone of infarction, indicating increased integrin  $\alpha_v\beta_3$  expression (Fig. 4) [52•, 81, 82].

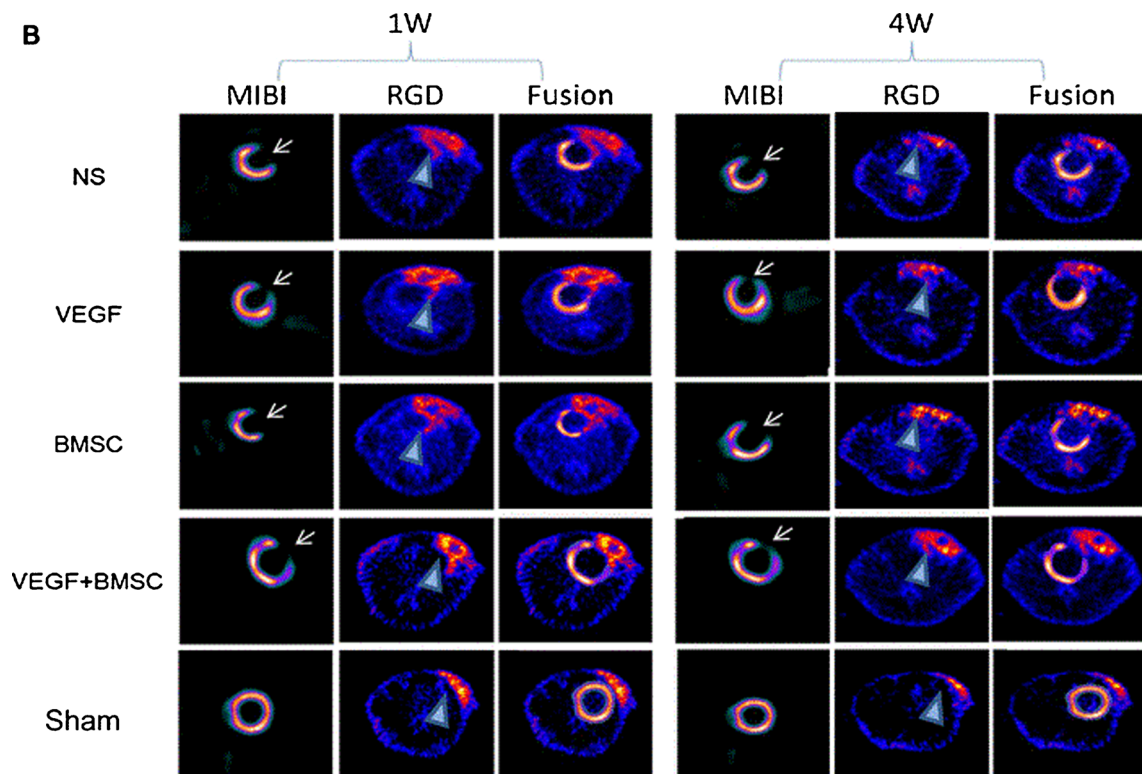
Recently, a  $^{68}\text{Ga}$ -labeled cyclic RGD dimer with a PEG spacer ( $^{68}\text{Ga}$ -PRGD2) was studied for the first time in a small set of patients post-MI.  $^{68}\text{Ga}$ -PRGD2 uptake was found in 20 of 23 patients around the ischemic regions. Increased uptake was found 1 week after MI and remained high until 2.5 months after MI.  $^{68}\text{Ga}$ -PRGD2 uptake correlated with size and severity of the infarction (Fig. 5). Three patients who did not show any  $^{68}\text{Ga}$ -PRGD2 uptake were identified with a very recent MI and events dated back 1–2 years. Nevertheless,  $^{68}\text{Ga}$ -PRGD2 uptake showed a patchy pattern, which may be attributable to an uptake not only by angiogenic ECs but also interstitial myofibroblasts contributing to myocardial remodeling [55••]. Although the application of integrin  $\alpha_v\beta_3$  imaging has been previously translated into clinical trials to assess tumor angiogenesis [83], only a single clinical trial imaging angiogenesis after MI has been conducted so far, with two studies currently recruiting (NCT01813045, NCT01542073).

Even though recent work in integrin  $\alpha_v\beta_3$  imaging with PET or SPECT registered substantial improvements, this method is still afflicted with several limitations. Recently, a cyclic RGD moiety conjugated to MPIO (c(RGDyK)-MPIO) for MR angiogenesis visualization in a colorectal carcinoma and melanoma mouse model was studied. c(RGDyK)-MPIO specifically binds to integrin  $\alpha_v\beta_3$  expressing vessels, while unbound particles are rapidly cleared from circulation. Specific binding was verified by ex vivo immunolabeling [56•]. Further optimization of MR-based angiogenesis imaging tracers may enable integrated molecular and anatomical imaging.

CEU imaging with targeted microbubbles displays another radiation-free molecular imaging technique. Microbubbles binding to integrin  $\alpha_v\beta_3$  and other angiogenesis specific targets have been extensively applied for studying angiogenesis and the response to antiangiogenic therapies in several tumor entities [35, 84–86]. However, only limited data exist regarding cardiovascular diseases and treatments [87]. Xie et al. investigated the effect of HIF-1 $\alpha$  mutant on angiogenesis in a mouse ischemic hind limb model; CEU imaging using  $\alpha_v$ -integrin-coated microbubbles has been applied to visualize angiogenesis. Video intensity obtained by  $\alpha_v$  imaging positively correlated with ultrasound perfusion imaging data, indicating that CEU imaging may also provide quantitative data

**Fig. 2** Macrosections and microsections of rat hearts. [...] d, e Representative immunostaining for CD61 (d) and CD31 (e) from the border region of infarcted heart at low magnification ( $\times 10$ , calibration bar 50  $\mu\text{m}$ ) (reprinted from [51] with permission from Springer/European Journal of Nuclear Medicine)

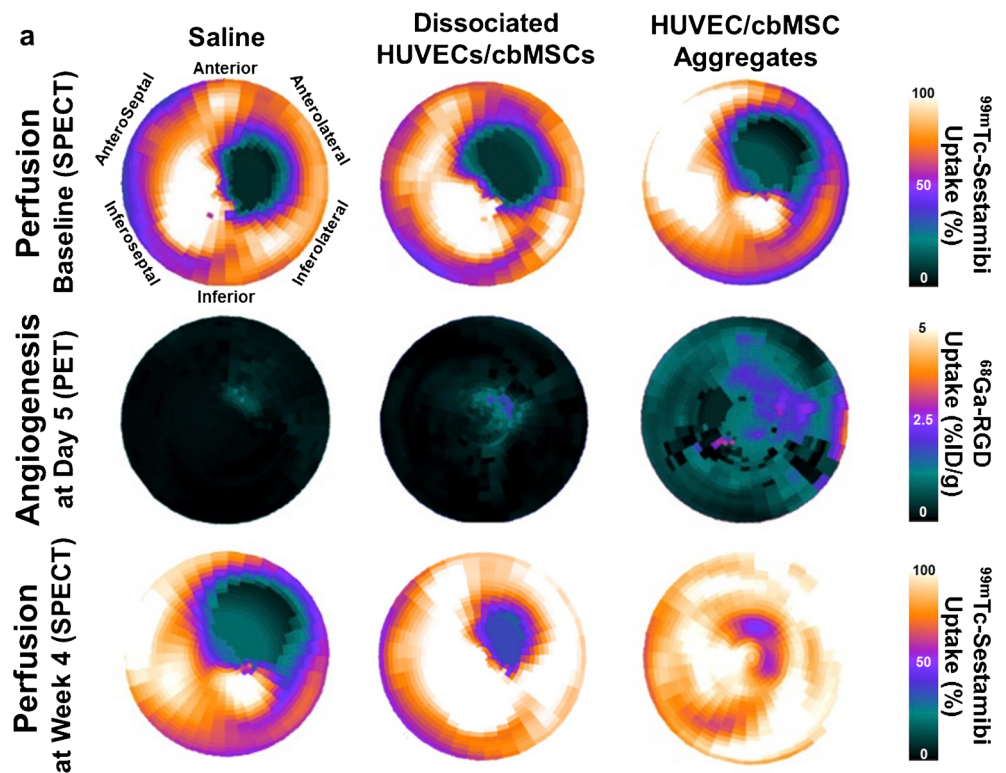




**Fig. 3** [...] **b** In vivo PET images of 18F-Alfatide II and representative SPECT myocardial short axis slice images using 99mTc-MIBI at different times after myocardial infarction. Infarcted myocardium showed obvious 99mTc-MIBI uptake defect in the anterior and lateral

wall of left ventricle (*arrows*), which matched the focal RGD peptide tracer uptake region (*triangle*). **c** The infarct area/remote area ratio of 18F-Alfatide II uptake as measured by PET (reprinted from [20•] with permission from Springer)

**Fig. 4** Multimodality noninvasive imaging by SPECT and PET, showing myocardial perfusion and angiogenesis, respectively. **a** SPECT and PET images in polar-map format, showing perfusion defects and angiogenesis of infarcted hearts that were treated with saline, dissociated cells, or cell aggregates. [...] (reprinted from [52•] with permission from Elsevier)



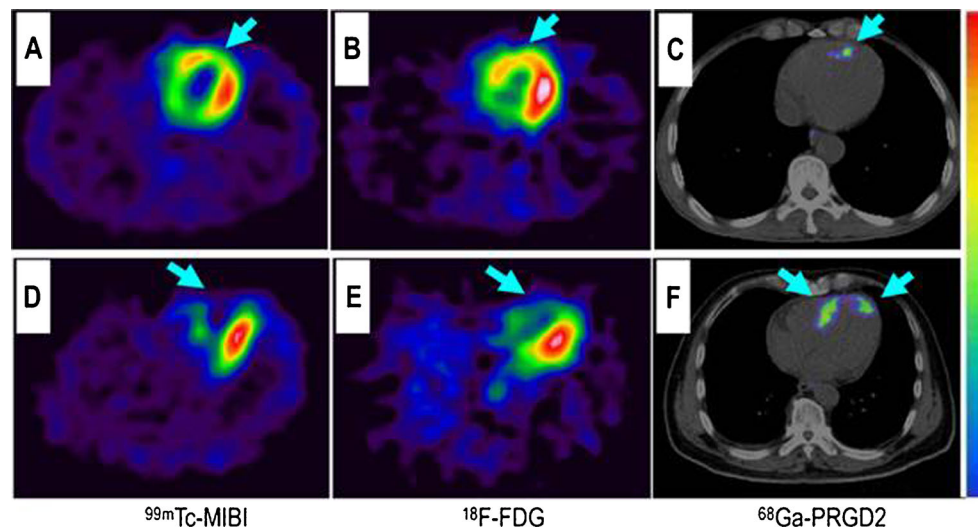


**Fig. 5** Comparison of a patient with slight myocardial infarction (MI) and a patient with severe MI. *Upper row:* In a 58-year-old man at the fifth day after the event, a small apical region with decreased  $^{99m}\text{Tc}$ -MIBI perfusion (**a**, arrow) and  $^{18}\text{F}$ -FDG metabolism (**b**, arrow) showed mild  $^{68}\text{Ga}$ -PRGD2 accumulation (**c**, arrow), with a pSUV of 0.62. *Lower row:*

In a 45-year-old woman on the seventh day after the event, an apical defect on  $^{99m}\text{Tc}$ -MIBI perfusion images (**d**, arrow) and  $^{18}\text{F}$ -FDG metabolism images (**e**, arrow) corresponded with moderate  $^{68}\text{Ga}$ -PRGD2 uptake (**f**, arrows), with a pSUV of 2.02 (reprinted from [55••] with permission from Theranostics)

on angiogenesis. This suggests that  $\alpha_v$ -integrin imaging via ultrasound can be a reliable method to visualize angiogenesis in vivo [34]. Moreover, ultrasound is not only limited to imaging angiogenesis to monitor cardiac regeneration but offers therapeutic options. Microbubbles loaded with therapeutic agents can be dissolved by high acoustic pressures after accumulation at the region of interest, thus enabling targeted drug delivery. Additionally, it is hypothesized that a combination of targeted imaging and drug release via microbubbles is possible [33, 88, 89].

### Integrin $\alpha_5\beta_1$

Integrin  $\alpha_5\beta_1$  expression is suggested to be completely restricted to ECs as deletion of the  $\beta_1$  chain leads to full inhibition of angiogenesis [90]. Analogous to integrin  $\alpha_v\beta_3$ , expression of integrin  $\alpha_5\beta_1$  is low in quiescent ECs and upregulated in angiogenic ECs [91, 92]. These results suggest that integrin  $\alpha_5\beta_1$  could be a more reliable biomarker for angiogenesis compared to  $\alpha_v\beta_3$ . To assess integrin  $\alpha_5\beta_1$  imaging in tumor angiogenesis, Notni et al. developed  $^{68}\text{Ga}$ -aquibepirin (a pseudopeptide targeting integrin  $\alpha_5\beta_1$ ) and compared it to  $^{68}\text{Ga}$ -avebetrin (targeting integrin  $\alpha_v\beta_3$ ). In vitro data showed high affinity for integrin  $\alpha_5\beta_1$ , and no decrease in specificity compared to a previously used  $^{68}\text{Ga}$ -labeled monomer selectively targeting integrin  $\alpha_5\beta_1$  was detected. In vivo data showed a higher tumor-to-organ ratio of  $^{68}\text{Ga}$ -aquibepirin and suggest it to be sufficiently stable. Immunohistochemical stainings further propose integrin  $\alpha_5\beta_1$  as a more EC specific marker [57••].

### Other targets for molecular imaging

#### CD13

CD13 is a membrane-bound aminopeptidase, which is upregulated on activated ECs [93]. It is considered an important regulator of EC morphogenesis during angiogenesis [94]. The cyclic tripeptide Asn-Gly-Arg (cNGR) binds to CD13 on activated ECs in infarcted myocardium, but not to CD13-positive macrophages in hypoxic myocardium [53, 95]. Comparative studies with RGD and NGR of tumor angiogenesis revealed a threefold higher target homing ratio for NGR [96]. A recent study investigated CD13-targeted angiogenesis imaging in a mouse model of MI with  $^{111}\text{In}$ -DTPA-cNGR by SPECT. Increased uptake of  $^{111}\text{In}$ -DTPA-cNGR at day 7 after MI correlated with areas of decreased  $^{99m}\text{Tc}$ -sestamibi [53].

#### CD105

CD105 (endoglin) is a transmembrane protein that is solely expressed on activated ECs [97]. Several PET probes based on TRC105, a monoclonal antibody that binds to CD105 with high avidity, have been tested for tumor angiogenesis imaging [98, 99].  $^{64}\text{Cu}$ -NOTA-TRC105 was recently tested to assess angiogenesis in a rat MI model via PET. Tracer uptake was increased in infarcted myocardium. Expression of CD105 was confirmed by immunofluorescence. However,  $^{64}\text{Cu}$ -NOTA-TRC105 exhibits a long half-life and its intense background signal acted as a confounder [54].

## VEGF

VEGF is commonly considered as the most potent mediator of angiogenesis. Consequently, VEGF and its receptors (VEGFRs) are frequently used for angiogenesis imaging. Due to splice variants, several isoforms of VEGF-A exist, of which some are proangiogenic and other antiangiogenic [100]. Monoclonal human anti-VEGF labeled with  $^{123}\text{I}$  and  $^{124}\text{I}$  have been employed for PET/SPECT imaging [101]. In a rat model of myocardial infarction, recombinant radiolabeled VEGF ( $^{64}\text{Cu}$ -DOTA-VEGF<sub>121</sub>) was used for PET imaging of VEGFRs. An increased radiotracer uptake was reported in a period of up to 2 weeks after induction of MI [101].

Several tyrosine kinases are upregulated in heart tissue undergoing angiogenesis and remodeling after MI. Immunohistochemical analyses of MI samples revealed increased levels of VEGFR-2, Tie-2, and PDGF $\alpha$  suggesting its use as an angiogenesis marker in non-invasive molecular imaging. ATV-1 can act as an inhibitor of those kinases. PET imaging with [ $^{11}\text{C}$ ]ATV-1 was assessed in a rat model of MI. Standard uptake values of [ $^{11}\text{C}$ ]ATV-1 correlated with immunohistochemical staining of VEGFR-2, Tie-2, and PDGF $\alpha$  [9].

## Conclusions

Even though proangiogenic therapies have so far largely failed as an effective treatment of MI, targeting angiogenesis after MI to mitigate heart failure is still considered a promising strategy. In order to assess the success of such therapeutic interventions in the clinic or in preclinical development, reliable and sensitive noninvasive imaging modalities are needed. Molecular imaging of angiogenesis via PET, SPECT, MRI, and CEU has been investigated intensively within the past decade. A variety of tracers have been translated from tumor angiogenesis models to MI models, and promising results were achieved. These methods offer the unique opportunity to study in vivo molecular mechanisms characterizing myocardial healing after infarction and to evaluate angiogenic effects of regenerative treatments. Combination of high sensitivity PET and SPECT with high-resolution X-ray CT images allows better identification and quantification of tracer uptake within the region of interest. Multimodal imaging with highly specific tracers yields reliable and detailed data of cardiac angiogenesis in small and large animal models and also in humans. Because PET and SPECT imaging use ionizing radiation, these imaging modalities might also expose patients to a risk of growing neoplastic lesions. For clinical applications, further research is warranted to develop radiotracers with a reasonable level of ionizing radiation or even replacing PET and SPECT with MRI or CEU while still featuring high affinity for visualizing growing blood vessels. Continuing development of noninvasive imaging modalities for future clinical

applications may enable improved patient risk stratification and pave the way for personalized therapy.

**Acknowledgments** Open access funding provided by Medical University of Vienna.

## Compliance with Ethics Standards

**Conflict of Interest** The authors declare that they have no conflict of interest.

**Human and Animal Rights and Informed Consent** This article does not contain any studies with human or animal subjects performed by any of the authors.

**Open Access** This article is distributed under the terms of the Creative Commons Attribution 4.0 International License (<http://creativecommons.org/licenses/by/4.0/>), which permits unrestricted use, distribution, and reproduction in any medium, provided you give appropriate credit to the original author(s) and the source, provide a link to the Creative Commons license, and indicate if changes were made.

## References

Papers of particular interest, published recently, have been highlighted as:

- Of importance
- Of major importance

1. Cochain C, Channon KM, Silvestre JS. Angiogenesis in the infarcted myocardium. *Antioxid Redox Signal*. 2013;18(9):1100–13. doi:10.1089/ars.2012.4849.
2. Shah AM, Mann DL. In search of new therapeutic targets and strategies for heart failure: recent advances in basic science. *Lancet*. 2011;378(9792):704–12. doi:10.1016/S0140-6736(11)60894-5.
3. Battegay EJ. Angiogenesis: mechanistic insights, neovascular diseases, and therapeutic prospects. *J Mol Med*. 1995;73(7):333–46.
4. Meoli DF, Sadeghi MM, Krassilnikova S, Bourke BN, Giordano FJ, Dione DP, et al. Noninvasive imaging of myocardial angiogenesis following experimental myocardial infarction. *J Clin Invest*. 2004;113(12):1684–91. doi:10.1172/JCI20352.
5. Uchida Y, Yanagisawa-Miwa A, Nakamura F, Yamada K, Tomaru T, Kimura K, et al. Angiogenic therapy of acute myocardial infarction by intrapericardial injection of basic fibroblast growth factor and heparin sulfate: an experimental study. *Am Heart J*. 1995;130(6):1182–8.
6. Gyöngyösi M, Wojakowski W, Lemarchand P, Lunde K, Tendera M, Bartunek J, et al. Meta-analysis of cell-based CaRdiac stUdiEs (ACCRUE) in patients with acute myocardial infarction based on individual patient data. *Circ Res*. 2015. doi:10.1161/circresaha.116.304346.
7. Scimia MC, Gumpert AM, Koch WJ. Cardiovascular gene therapy for myocardial infarction. *Expert Opin Biol Ther*. 2014;14(2):183–95. doi:10.1517/14712598.2014.866085.
8. Potente M, Gerhardt H, Carmeliet P. Basic and therapeutic aspects of angiogenesis. *Cell*. 2011;146(6):873–87. doi:10.1016/j.cell.2011.08.039.
9. Dissoki S, Abourbeh G, Salnikov O, Mishani E, Jacobson O. PET molecular imaging of angiogenesis with a multiple tyrosine kinase receptor-targeted agent in a rat model of myocardial infarction. *Mol Imaging Biol*. 2015;17(2):222–30. doi:10.1007/s11307-014-0790-8.



10. Carmeliet P, Jain RK. Molecular mechanisms and clinical applications of angiogenesis. *Nature*. 2011;473(7347):298–307. doi:10.1038/nature10144.
11. Frangogiannis NG. The mechanistic basis of infarct healing. *Antioxid Redox Signal*. 2006;8(11-12):1907–39. doi:10.1089/ars.2006.8.1907.
12. Cohn JN, Ferrari R, Sharpe N. Cardiac remodeling—concepts and clinical implications: a consensus paper from an international forum on cardiac remodeling. Behalf of an International Forum on Cardiac Remodeling. *J Am Coll Cardiol*. 2000;35(3):569–82.
13. Shiojima I, Sato K, Izumiya Y, Schiekofe S, Ito M, Liao R, et al. Disruption of coordinated cardiac hypertrophy and angiogenesis contributes to the transition to heart failure. *J Clin Invest*. 2005;115(8):2108–18. doi:10.1172/JCI24682.
14. Silvestre JS, Smadja DM, Levy BI. Postischemic revascularization: from cellular and molecular mechanisms to clinical applications. *Physiol Rev*. 2013;93(4):1743–802. doi:10.1152/physrev.00006.2013.
15. Jivraj N, Phinikaridou A, Shah AM, Botnar RM. Molecular imaging of myocardial infarction. *Basic Res Cardiol*. 2014;109(1):397. doi:10.1007/s00395-013-0397-2.
16. Stacy MR, Sinusas AJ. Emerging imaging modalities in regenerative medicine. *Curr Pathobiol Rep*. 2015;3(1):27–36. doi:10.1007/s40139-015-0073-3.
17. Ripa RS, Kjaer A. Imaging atherosclerosis with hybrid positron emission tomography/magnetic resonance imaging. *Biomed Res Int*. 2015;2015:914516. doi:10.1155/2015/914516.
18. Stacy MR, Maxfield MW, Sinusas AJ. Targeted molecular imaging of angiogenesis in PET and SPECT: a review. *Yale J Biol Med*. 2012;85(1):75–86.
19. Naumova AV, Modo M, Moore A, Murry CE, Frank JA. Clinical imaging in regenerative medicine. *Nat Biotechnol*. 2014;32(8):804–18. doi:10.1038/nbt.2993.
20. Cai M, Ren L, Yin X, Guo Z, Li Y, He T, Tang Y, Long T, Liu Y, Liu G, Zhang X, Hu S. PET monitoring angiogenesis of infarcted myocardium after treatment with vascular endothelial growth factor and bone marrow mesenchymal stem cells. *Amino Acids*. 2016; 48(3): 811–820. doi:10.1007/s00726-015-2129-4. **This experimental rat myocardial infarction model introduces a new <sup>18</sup>F based radiotracer for angiogenesis imaging which offers a variety of advantages over previous radiotracers. Moreover, <sup>18</sup>F-Alfatide II was used to demonstrate increased myocardial angiogenesis in rats treated with VEGF and/or BMSCs.**
21. Li X, Heber D, Rausch I, Beitzke D, Mayerhoefer ME, Rasul S, et al. Quantitative assessment of atherosclerotic plaques on F-FDG PET/MRI: comparison with a PET/CT hybrid system. *Eur J Nucl Med Mol Imaging*. 2016. doi:10.1007/s00259-016-3308-6.
22. Ratib O, Nkoulou R. Potential applications of PET/MR imaging in cardiology. *J Nucl Med*. 2014;55(Supplement 2):40S–6. doi:10.2967/jnumed.113.129262.
23. Stacy MR, Paeng JC, Sinusas AJ. The role of molecular imaging in the evaluation of myocardial and peripheral angiogenesis. *Ann Nucl Med*. 2015;29(3):217–23. doi:10.1007/s12149-015-0961-y.
24. Lee JS, Kim JH. Recent advances in hybrid molecular imaging systems. *Semin Musculoskelet Radiol*. 2014;18(2):103–22. doi:10.1055/s-0034-1371014.
25. Constantine G, Shan K, Flamm SD, Sivananthan MU. Role of MRI in clinical cardiology. *Lancet*. 2004;363(9427):2162–71. doi:10.1016/S0140-6736(04)16509-4.
26. Mulder WJ, Strijkers GJ, Habets JW, Bleeker EJ, van der Schaft DW, Storm G, et al. MR molecular imaging and fluorescence microscopy for identification of activated tumor endothelium using a bimodal lipidic nanoparticle. *FASEB J*. 2005;19(14):2008–10. doi:10.1096/fj.05-4145fje.
27. Schmieder AH, Winter PM, Caruthers SD, Harris TD, Williams TA, Allen JS, et al. Molecular MR imaging of melanoma angiogenesis with alphanubeta3-targeted paramagnetic nanoparticles. *Magn Reson Med*. 2005;53(3):621–7. doi:10.1002/mrm.20391.
28. Sipkins DA, Cheresch DA, Kazemi MR, Nevin LM, Bednarski MD, Li KC. Detection of tumor angiogenesis in vivo by alphaVbeta3-targeted magnetic resonance imaging. *Nat Med*. 1998;4(5):623–6.
29. Zhang C, Jugold M, Woenne EC, Lammers T, Morgenstern B, Mueller MM, et al. Specific targeting of tumor angiogenesis by RGD-conjugated ultrasmall superparamagnetic iron oxide particles using a clinical 1.5-T magnetic resonance scanner. *Cancer Res*. 2007;67(4):1555–62. doi:10.1158/0008-5472.CAN-06-1668.
30. Leung K. Cyclo(Arg-Gly-Asp-D-Try-Glu) conjugated to ultrasmall superparamagnetic iron oxide nanoparticles. Bethesda (MD): Molecular Imaging and Contrast Agent Database (MICAD); 2004.
31. Yang Y, Yang Y, Yanasak N, Schumacher A, Hu TC. Temporal and noninvasive monitoring of inflammatory-cell infiltration to myocardial infarction sites using micrometer-sized iron oxide particles. *Magn Reson Med*. 2010;63(1):33–40. doi:10.1002/mrm.22175.
32. Singh N, Jenkins GJS, Asadi R, Doak SH. Potential toxicity of superparamagnetic iron oxide nanoparticles (SPION). *Nano Reviews*. 2010; 1:10.3402/nano.v3401i3400.5358. doi:10.3402/nano.v1i0.5358.
33. Smith AH, Fujii H, Kuliszewski MA, Leong-Poi H. Contrast ultrasound and targeted microbubbles: diagnostic and therapeutic applications for angiogenesis. *J Cardiovasc Transl Res*. 2011;4(4):404–15. doi:10.1007/s12265-011-9282-2.
34. Xie J, Liao Y, Yang L, Wu J, Liu C, Xuan W, et al. Ultrasound molecular imaging of angiogenesis induced by mutant forms of hypoxia-inducible factor-1alpha. *Cardiovasc Res*. 2011;92(2):256–66. doi:10.1093/cvr/cvr229.
35. Payen T, Dizeux A, Baldini C, Le Guillou-Buffello D, Lamuraglia M, Comperat E, et al. VEGFR2-targeted contrast-enhanced ultrasound to distinguish between two anti-angiogenic treatments. *Ultrasound Med Biol*. 2015;41(8):2202–11. doi:10.1016/j.ultrasmedbio.2015.04.010.
36. Kim JE, Kalimuthu S, Ahn BC. In vivo cell tracking with bioluminescence imaging. *Nucl Med Mol Imaging*. 2015;49(1):3–10. doi:10.1007/s13139-014-0309-x.
37. Baker M. Whole-animal imaging: the whole picture. *Nature*. 2010;463(7283):977–80. doi:10.1038/463977a.
38. Ahn BC. Applications of molecular imaging in drug discovery and development process. *Curr Pharm Biotechnol*. 2011;12(4):459–68.
39. Nguyen PK, Lan F, Wang Y, Wu JC. Imaging: guiding the clinical translation of cardiac stem cell therapy. *Circ Res*. 2011;109(8):962–79. doi:10.1161/CIRCRESAHA.111.242909.
40. Blankstein R, Di Carli MF. Integration of coronary anatomy and myocardial perfusion imaging. *Nat Rev Cardiol*. 2010;7(4):226–36. doi:10.1038/nrcardio.2010.15.
41. Gaemperli O, Kaufmann PA, Alkadhi H. Cardiac hybrid imaging. *Eur J Nucl Med Mol Imaging*. 2014;41 Suppl 1:S91–103. doi:10.1007/s00259-013-2566-9.
42. Fricke E, Fricke H, Weise R, Kammeier A, Hagedorn R, Lotz N, et al. Attenuation correction of myocardial SPECT perfusion images with low-dose CT: evaluation of the method by comparison with perfusion PET. *J Nucl Med*. 2005;46(5):736–44.
43. Brown ER, Kronmal RA, Bluemke DA, Guerci AD, Carr JJ, Goldin J, et al. Coronary calcium coverage score: determination, correlates, and predictive accuracy in the Multi-Ethnic Study of Atherosclerosis. *Radiology*. 2008;247(3):669–75. doi:10.1148/radiol.2473071469.
44. Budoff MJ, Shaw LJ, Liu ST, Weinstein SR, Mosler TP, Tseng PH, et al. Long-term prognosis associated with coronary calcification: observations from a registry of 25,253 patients. *J Am Coll Cardiol*. 2007;49(18):1860–70. doi:10.1016/j.jacc.2006.10.079.

45. Henzlova MJ, Duvall WL. The future of SPECT MPI: time and dose reduction. *J Nucl Cardiol*. 2011;18(4):580–7. doi:10.1007/s12350-011-9401-0.
46. Palyo R, Sinusas A, Liu YH. High-sensitivity and high-resolution SPECT/CT systems provide substantial dose reduction without compromising quantitative precision for assessment of myocardial perfusion or function. *J Nucl Med*. 2016. doi:10.2967/jnumed.115.164632.
47. Joshi NV, Vesey AT, Williams MC, Shah AS, Calvert PA, Craighead FH, et al. 18F-fluoride positron emission tomography for identification of ruptured and high-risk coronary atherosclerotic plaques: a prospective clinical trial. *Lancet*. 2014;383(9918):705–13. doi:10.1016/S0140-6736(13)61754-7.
48. Mazurek T, Kobylecka M, Zielonkiewicz M, Kurek A, Kochman J, Filipiak KJ, et al. PET/CT evaluation of F-FDG uptake in pericoronary adipose tissue in patients with stable coronary artery disease: Independent predictor of atherosclerotic lesions' formation? *J Nucl Cardiol*. 2016. doi:10.1007/s12350-015-0370-6.
49. Iagaru A, Gambhir SS. Imaging tumor angiogenesis: the road to clinical utility. *AJR Am J Roentgenol*. 2013;201(2):W183–91. doi:10.2214/AJR.12.8568.
50. Laitinen I, Notni J, Pohle K, Rudelius M, Farrell E, Nekolla SG, et al. Comparison of cyclic RGD peptides for alphavbeta3 integrin detection in a rat model of myocardial infarction. *EJNMMI Res*. 2013;3(1):38. doi:10.1186/2191-219x-3-38.
51. Menichetti L, Kusmic C, Panetta D, Arosio D, Petroni D, Matteucci M, et al. MicroPET/CT imaging of alphavbeta(3) integrin via a novel (6)(8)Ga-NOTA-RGD peptidomimetic conjugate in rat myocardial infarction. *Eur J Nucl Med Mol Imaging*. 2013;40(8):1265–74. doi:10.1007/s00259-013-2432-9.
52. Huang CC, Wei HJ, Lin KJ, Lin WW, Wang CW, Pan WY, Hwang SM, Chang Y, Sung HW. Multimodality noninvasive imaging for assessing therapeutic effects of exogenously transplanted cell aggregates capable of angiogenesis on acute myocardial infarction. *Biomaterials*. 2015; 73:12–22. doi:10.1016/j.biomaterials.2015.09.009. **This is an experimental rat MI study showing that the application of 3D aggregates of HUVECs/cbMSCs improves blood perfusion and global/regional ventricular function. Additionally those aggregates induced increased angiogenesis which was shown in vivo using non-invasive angiogenesis imaging by PET targeting integrin  $\alpha_v\beta_3$  and immunohistochemical stainings.**
53. Hendriks G, De Saint-Hubert M, Dijkgraaf I, Bauwens M, Douma K, Wierts R, et al. Molecular imaging of angiogenesis after myocardial infarction by (111)In-DTPA-cNGR and (99m)Tc-sestamibi dual-isotope myocardial SPECT. *EJNMMI Res*. 2015;5:2. doi:10.1186/s13550-015-0081-7.
54. Orbay H, Zhang Y, Valdovinos HF, Song G, Hernandez R, Theuer CP, et al. Positron emission tomography imaging of CD105 expression in a rat myocardial infarction model with (64)Cu-NOTA-TRC105. *Am J Nucl Med Mol Imaging*. 2013;4(1):1–9.
55. Sun Y, Zeng Y, Zhu Y, Feng F, Xu W, Wu C, Xing B, Zhang W, Wu P, Cui L, Wang R, Li F, Chen X, Zhu Z. Application of (68)Ga-PRGD2 PET/CT for alphavbeta3-integrin imaging of myocardial infarction and stroke. *Theranostics*. 2014; 4(8):778–786. doi:10.7150/thno.8809. **This trial is the first larger trial in humans on angiogenesis after myocardial infarction. It offers an insight into the role of angiogenesis through myocardial healing after infarction and provides evidence that PET imaging of integrin  $\alpha_v\beta_3$  is feasible.**
56. Melemenidis S, Jefferson A, Ruparelia N, Akhtar AM, Xie J, Allen D, et al. Molecular magnetic resonance imaging of angiogenesis in vivo using polyvalent cyclic RGD-iron oxide microparticle conjugates. *Theranostics*. 2015;5(5):515–29. doi:10.7150/thno.10319. **This study on tumour angiogenesis in mice shows for the first time representative in vivo angiogenesis imaging using RGD-targeted MPIOs in MRI.**
57. Notni J, Steiger K, Hoffmann F, Reich D, Kapp TG, Rechenmacher F, Neubauer S, Kessler H, Wester HJ. Complementary, selective PET imaging of integrin subtypes alpha5beta1 and alphavbeta3 using 68Ga-aquibepirin and 68Ga-avebetrin. *J Nucl Med*. 2016; 57(3):460–466. doi:10.2967/jnumed.115.165720. **This trial compares for the first time molecular imaging of myocardial angiogenesis in rat with MI two integrin subtypes. The so far rather neglected integrin  $\alpha_5\beta_1$  was demonstrated to be more specific for activated endothelial cells with however no decline in affinity.**
58. Dobrucki LW, de Muinck ED, Lindner JR, Sinusas AJ. Approaches to multimodality imaging of angiogenesis. *J Nucl Med*. 2010. doi:10.2967/jnumed.110.074963.
59. Luo BH, Springer TA. Integrin structures and conformational signaling. *Curr Opin Cell Biol*. 2006;18(5):579–86. doi:10.1016/j.ceb.2006.08.005.
60. Humphries MJ. Integrin cell adhesion receptors and the concept of agonism. *Trends Pharmacol Sci*. 2000;21(1):29–32.
61. Horton MA. The alpha v beta 3 integrin “vitronectin receptor”. *Int J Biochem Cell Biol*. 1997;29(5):721–5.
62. Higuchi T, Bengel FM, Seidl S, Watzlowik P, Kessler H, Hegenloh R, et al. Assessment of alphavbeta3 integrin expression after myocardial infarction by positron emission tomography. *Cardiovasc Res*. 2008;78(2):395–403. doi:10.1093/cvr/cvn033.
63. Bader BL, Rayburn H, Crowley D, Hynes RO. Extensive vasculogenesis, angiogenesis, and organogenesis precede lethality in mice lacking all alpha v integrins. *Cell*. 1998;95(4):507–19.
64. Reynolds LE, Wyder L, Lively JC, Taverna D, Robinson SD, Huang X, et al. Enhanced pathological angiogenesis in mice lacking beta3 integrin or beta3 and beta5 integrins. *Nat Med*. 2002;8(1):27–34. doi:10.1038/nm0102-27.
65. Reynolds AR, Reynolds LE, Nagel TE, Lively JC, Robinson SD, Hicklin DJ, et al. Elevated Flk1 (vascular endothelial growth factor receptor 2) signaling mediates enhanced angiogenesis in beta3-integrin-deficient mice. *Cancer Res*. 2004;64(23):8643–50. doi:10.1158/0008-5472.CAN-04-2760.
66. Atkinson SJ, Ellison TS, Steri V, Gould E, Robinson SD. Redefining the role(s) of endothelial alphavbeta3-integrin in angiogenesis. *Biochem Soc Trans*. 2014;42(6):1590–5. doi:10.1042/BST20140206.
67. Mitra ES, Goris ML, Iagaru AH, Kardan A, Burton L, Berganos R, et al. Pilot pharmacokinetic and dosimetric studies of (18)F-FPPRGD2: a PET radiopharmaceutical agent for imaging alpha(v)beta(3) integrin levels. *Radiology*. 2011;260(1):182–91. doi:10.1148/radiol.11101139.
68. Beer AJ, Lorenzen S, Metz S, Herrmann K, Watzlowik P, Wester HJ, et al. Comparison of integrin alphaVbeta3 expression and glucose metabolism in primary and metastatic lesions in cancer patients: a PET study using 18F-galacto-RGD and 18F-FDG. *J Nucl Med*. 2008;49(1):22–9. doi:10.2967/jnumed.107.045864.
69. Lang L, Li W, Guo N, Ma Y, Zhu L, Kiesewetter DO, et al. Comparison study of [18F]FA1-NOTA-PRGD2, [18F]FPPRGD2, and [68Ga]Ga-NOTA-PRGD2 for PET imaging of U87MG tumors in mice. *Bioconjug Chem*. 2011;22(12):2415–22. doi:10.1021/bc200197h.
70. Zhu Z, Yin Y, Zheng K, Li F, Chen X, Zhang F, et al. Evaluation of synovial angiogenesis in patients with rheumatoid arthritis using (6)(8)Ga-PRGD2 PET/CT: a prospective proof-of-concept cohort study. *Ann Rheum Dis*. 2014;73(6):1269–72. doi:10.1136/annrheumdis-2013-204820.
71. Chen X, Liu S, Hou Y, Tohme M, Park R, Bading JR, et al. MicroPET imaging of breast cancer alphav-integrin expression with 64Cu-labeled dimeric RGD peptides. *Mol Imaging Biol*. 2004;6(5):350–9. doi:10.1016/j.mibio.2004.06.004.

72. Lang L, Li W, Jia HM, Fang DC, Zhang S, Sun X, et al. New methods for labeling RGD peptides with bromine-76. *Theranostics*. 2011;1:341–53.
73. Jacobson O, Zhu L, Niu G, Weiss ID, Szajek LP, Ma Y, et al. MicroPET imaging of integrin alphavbeta3 expressing tumors using 89Zr-RGD peptides. *Mol Imaging Biol*. 2011;13(6):1224–33. doi:10.1007/s11307-010-0458-y.
74. Axelsson R, Bach-Gansmo T, Castell-Conesa J, McParland BJ, Study G. An open-label, multicenter, phase 2a study to assess the feasibility of imaging metastases in late-stage cancer patients with the alpha v beta 3-selective angiogenesis imaging agent 99mTc-NC100692. *Acta Radiol*. 2010;51(1):40–6. doi:10.3109/02841850903273974.
75. Jia B, Liu Z, Zhu Z, Shi J, Jin X, Zhao H, et al. Blood clearance kinetics, biodistribution, and radiation dosimetry of a kit-formulated integrin alphavbeta3-selective radiotracer 99mTc-3PRGD 2 in non-human primates. *Mol Imaging Biol*. 2011;13(4):730–6. doi:10.1007/s11307-010-0385-y.
76. Terry SY, Abiraj K, Frielink C, van Dijk LK, Bussink J, Oyen WJ, et al. Imaging integrin alphavbeta3 on blood vessels with 111In-RGD2 in head and neck tumor xenografts. *J Nucl Med*. 2014;55(2):281–6. doi:10.2967/jnumed.113.129668.
77. Sherif HM, Saraste A, Nekolla SG, Weidl E, Reder S, Tapfer A, et al. Molecular imaging of early alphavbeta3 integrin expression predicts long-term left-ventricle remodeling after myocardial infarction in rats. *J Nucl Med*. 2012;53(2):318–23. doi:10.2967/jnumed.111.091652.
78. Notni J, Pohle K, Wester HJ. Be spoilt for choice with radiolabelled RGD peptides: preclinical evaluation of (6)(8)Ga-TRAP(RGD)(3). *Nucl Med Biol*. 2013;40(1):33–41. doi:10.1016/j.nucmedbio.2012.08.006.
79. Pohle K, Notni J, Bussemer J, Kessler H, Schwaiger M, Beer AJ. 68Ga-NODAGA-RGD is a suitable substitute for (18)F-Galacto-RGD and can be produced with high specific activity in a cGMP/GRP compliant automated process. *Nucl Med Biol*. 2012;39(6):777–84. doi:10.1016/j.nucmedbio.2012.02.006.
80. Gao H, Lang L, Guo N, Cao F, Quan Q, Hu S, et al. PET imaging of angiogenesis after myocardial infarction/reperfusion using a one-step labeled integrin targeted tracer (18)F-AIF-NOTA-PRGD2. *Eur J Nucl Med Mol Imaging*. 2012;39(4):683–92. doi:10.1007/s00259-011-2052-1.
81. Dimastromatteo J, Riou LM, Ahmadi M, Pons G, Pellegrini E, Broisat A, et al. In vivo molecular imaging of myocardial angiogenesis using the  $\alpha v \beta 3$  integrin-targeted tracer 99mTc-RAFT-RGD. *J Nucl Cardiol*. 2010;17(3):435–43. doi:10.1007/s12350-010-9191-9.
82. Paeng JC, Bregasi A, Sahul Z, Kalinowski L, Dobrucki LW, Brennan M, et al. Serial reference tissue-based quantitative and volumetric analysis of integrin-targeted angiogenesis imaging: chronic canine model of myocardial infarction. *J Nucl Med*. 2014;2014(55):1710.
83. Gaertner FC, Kessler H, Wester HJ, Schwaiger M, Beer AJ. Radiolabelled RGD peptides for imaging and therapy. *Eur J Nucl Med Mol Imaging*. 2012;39 Suppl 1:S126–38. doi:10.1007/s00259-011-2028-1.
84. Hu Q, Wang XY, Kang LK, Wei HM, Xu CM, Wang T, et al. RGD-targeted ultrasound contrast agent for longitudinal assessment of Hep-2 tumor angiogenesis in vivo. *PLoS One*. 2016;11(2):e0149075. doi:10.1371/journal.pone.0149075.
85. Shelton SE, Lindsey BD, Tsuruta JK, Foster FS, Dayton PA. Molecular acoustic angiography: a new technique for high-resolution superharmonic ultrasound molecular imaging. *Ultrasound Med Biol*. 2016;42(3):769–81. doi:10.1016/j.ultrasmedbio.2015.10.015.
86. Yan F, Xu X, Chen Y, Deng Z, Liu H, Xu J, et al. A lipopeptide-based alphavbeta(3) integrin-targeted ultrasound contrast agent for molecular imaging of tumor angiogenesis. *Ultrasound Med Biol*. 2015;41(10):2765–73. doi:10.1016/j.ultrasmedbio.2015.05.023.
87. Leong-Poi H. Molecular imaging using contrast-enhanced ultrasound: evaluation of angiogenesis and cell therapy. *Cardiovasc Res*. 2009;84(2):190–200. doi:10.1093/cvr/cvp248.
88. Deng Q, Hu B, Cao S, Song HN, Chen JL, Zhou Q. Improving the efficacy of therapeutic angiogenesis by UTMD-mediated Ang-1 gene delivery to the infarcted myocardium. *Int J Mol Med*. 2015;36(2):335–44. doi:10.3892/ijmm.2015.2226.
89. Nguyen AT, Wrenn SP. Acoustically active liposome-nanobubble complexes for enhanced ultrasonic imaging and ultrasound-triggered drug delivery. *Wiley Interdiscip Rev Nanomed Nanobiotechnol*. 2014;6(3):316–25. doi:10.1002/wnan.1255.
90. Fassler R, Meyer M. Consequences of lack of beta 1 integrin gene expression in mice. *Genes Dev*. 1995;9(15):1896–908.
91. Tanjore H, Zeisberg EM, Gerami-Naini B, Kalluri R. Beta1 integrin expression on endothelial cells is required for angiogenesis but not for vasculogenesis. *Dev Dyn*. 2008;237(1):75–82. doi:10.1002/dvdy.21385.
92. Kim S, Bell K, Mousa SA, Varner JA. Regulation of angiogenesis in vivo by ligation of integrin alpha5beta1 with the central cell-binding domain of fibronectin. *Am J Pathol*. 2000;156(4):1345–62.
93. Corti A, Curnis F, Arap W, Pasqualini R. The neovasculature homing motif NGR: more than meets the eye. *Blood*. 2008;112(7):2628–35. doi:10.1182/blood-2008-04-150862.
94. Bhagwat SV, Lahdenranta J, Giordano R, Arap W, Pasqualini R, Shapiro LH. CD13/APN is activated by angiogenic signals and is essential for capillary tube formation. *Blood*. 2001;97(3):652–9.
95. Buehler A, van Zandvoort MA, Stelt BJ, Hackeng TM, Schrans-Stassen BH, Bennaghmouch A, et al. cNGR: a novel homing sequence for CD13/APN targeted molecular imaging of murine cardiac angiogenesis in vivo. *Arterioscler Thromb Vasc Biol*. 2006;26(12):2681–7. doi:10.1161/01.ATV.0000245807.65714.0b.
96. Arap W, Pasqualini R, Ruoslahti E. Cancer treatment by targeted drug delivery to tumor vasculature in a mouse model. *Science*. 1998;279(5349):377–80.
97. Fonsatti E, Sigalotti L, Arslan P, Altomonte M, Maio M. Emerging role of endoglin (CD105) as a marker of angiogenesis with clinical potential in human malignancies. *Curr Cancer Drug Targets*. 2003;3(6):427–32.
98. Hong H, Zhang Y, Orbay H, Valdovinos HF, Nayak TR, Bean J, et al. Positron emission tomography imaging of tumor angiogenesis with a (61/64)Cu-labeled F(ab')<sub>2</sub> antibody fragment. *Mol Pharm*. 2013;10(2):709–16. doi:10.1021/mp300507r.
99. Zhang Y, Hong H, Severin GW, Engle JW, Yang Y, Goel S, et al. ImmunoPET and near-infrared fluorescence imaging of CD105 expression using a monoclonal antibody dual-labeled with (89)Zr and IRDye 800CW. *Am J Transl Res*. 2012;4(3):333–46.
100. Nowak DG, Woolard J, Amin EM, Konopatskaya O, Saleem MA, Churchill AJ, et al. Expression of pro- and anti-angiogenic isoforms of VEGF is differentially regulated by splicing and growth factors. *J Cell Sci*. 2008;121(20):3487–95. doi:10.1242/jcs.016410.
101. Li S, Peck-Radosavljevic M, Koller E, Koller F, Kaserer K, Kreil A, et al. Characterization of 123I-vascular endothelial growth factor-binding sites expressed on human tumour cells: Possible implication for tumour scintigraphy. *Int J Cancer*. 2001;91(6):789–96. doi:10.1002/1097-0215(200002)9999:9999<::AID-IJC1126>3.0.CO;2-K.